Chapter 5

Estimation of Nanoporosity of ZSM-5 Zeolites as Hierarchical Materials

Miguel Angel Hernández, A. Abbaspourrad, Vitalli Petranovskii, Fernando Rojas, Roberto Portillo, Martha Alicia Salgado, Gabriela Hernández, Maria de los Angeles Velazco, Edgar Ayala and Karla Fabiola Quiroz

Additional information is available at the end of the chapter

http://dx.doi.org/10.5772/intechopen.73624

Abstract

The nanoporosity in zeolite ZSM-5 was analyzed as a function of SiO_2/Al_2O_3 molar ratio (MR). The internal pore structure was studied by high-resolution adsorption. Surface areas, microporous volume, characteristic energy of sorption, and pore-size distributions were calculated from N_2 sorption isotherms by the BET, Langmuir, *t*-method of de Boer, α_s-plot of Sing, direct comparative plots of Lee, Newnham, Dubinin-Astakhov, differential adsorption curves, and nonlocal density functional theory methods. The results indicated that MR dependence in these zeolites caused structural defects through micropore opening and widening as well as the emergence of further slit-like mesopores.

Keywords: ZSM-5 zeolite, sorption, nanopore measurements

1. Introduction

The nanoporous, ordered, and three-dimensional structure of zeolites makes them materials of great practical importance in the hierarchy. The broad use of microporous zeolites (pore diameter $w < 2$ nm) makes them very important in very specific areas, such as acid catalysts and adsorbents, as well as in refining processes and the basic petrochemical industry due to their unique properties both in activity and in selectivity [1]. The great majority of zeolites possess two types of porosity: primary and secondary. Primary porosity with a well-defined

size is associated with the crystalline structure of the zeolite and fundamentally depends on its structure type. Imperfections, including defects occurring during the growth of zeolite crystals, as well as defects generated by various treatments, cause secondary porosity, that is, the presence of mesopores ($2 < w < 50$ nm) and macropores ($w > 50$ nm) [2]. The secondary porosity differs from the framework porosity, since it does not directly depend on the crystalline structure of the zeolite. Taken together, these comprise the texture of a sorbent. The primary porosity is characterized by a microporous volume (W_0) with pore size as seen in the zeolite structure; secondary—by the pore-size distribution (PSD) and the external surface area (A_E). These parameters are usually calculated from nitrogen sorption isotherms [3]. Many, but not all, catalysts are porous materials, in which most of the surface area is internal. Sometimes it is convenient to talk about the structure and texture of such materials. The structure is defined both by the distribution in space of atoms or ions in the material part of the catalyst and by the distribution on the surface. The texture is defined by the detailed geometry of the void space in the catalyst particles. Porosity is a concept related to texture and refers to the porous space in the material. However, with zeolites, most of the porosity is determined by the crystal structure. To accurately describe the texture of the porous catalyst, a very large number of parameters will be required. With respect to porous solids, the surface associated with the pores can be called the internal surface. Since the availability of pores can depend on the ratio of the dimensions of the channel and molecules, the extent of the accessible internal surface may depend on the size of the molecules contained in the mixture and may be different for various components of the mixture (molecular sieve effect) [4].

ZSM-5 and, its purely siliceous analog, silicalite (both have a structural code "MFI" in accordance with the IZA database) are among the most widely studied zeolites. MFI is one of the most versatile and commercially significant zeolites; it is widely used in the petroleum industry to convert methanol into complex hydrocarbons in methanol-to-gasoline processes, as well as in the alkylation of aromatic compounds and their subsequent separation [5]. The microporous network of this zeolite consists of intersecting straight and sinusoidal channels. The straight channels have pore openings defined by a cross-section of 10-member rings of 0.54–0.57 nm and sinusoidal channels by elliptic pores of 0.51–0.54 nm in cross-section. The intersections are cavities of 0.8 nm in diameter [6] (see **Figure 1**).

A detailed study on the different types of adsorption sites that constitute the structural skeleton of this zeolite was carried out by Cho et al. [7]. They classified the sorption sites into three types: (1) the S_S sites located in straight channels; (2) the S_Z sites located in zigzag (sinusoidal) channels; and, finally, (3) the S_I sites located at the intersections (**Figure 2**). One of the most important catalytic properties of ZSM-5 is its shape selectivity. This is a consequence of its primary microporous structure and is the basis for most of its successful applications [8].

Another important parameter that allows to adjust the zeolite properties is their chemical composition, that is, their SiO_2/Al_2O_3 molar ratio (MR). The amount of Al in the framework is proportional to the number of exchangeable cations, H^+ among others, which affects both Lewis and Brønsted acidity. The main interactions of the sorbate molecules in the pores of the zeolite are realized through the oxygen atoms of the lattice and extra-framework cations. Microporosity and secondary porosity in zeolites and similar materials can be determined from the low- and medium-pressure regions of the sorption isotherm using various approaches [3]. The shape-selective activity of MFI can be attributed to the presence of active

http://dx.doi.org/10.5772/intechopen.73624

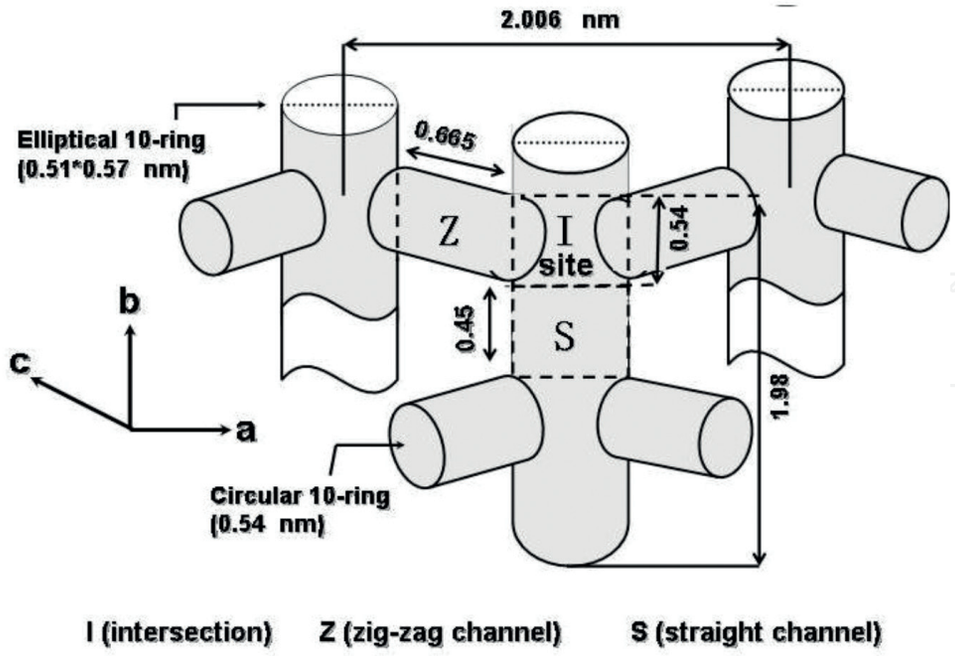

Figure 1. ZSM-5 zeolite structure. The dimensions of the pore channels are in nm. I, S, and Z are S_I, S_S, and S_Z sites, respectively.

sites in micropores. It was shown that the shape-selective properties of zeolites may be greatly reduced due to the presence of active sites in the secondary porosity with a wide distribution of the pore diameter and on the external surface of their crystallites, so zeolites with a large outer surface area are less selective than those with fewer imperfections.

The presence of molecules that blocks the pores of the zeolite or a partial destruction of its structure can drastically decrease its activity by reducing the microporous volume accessible for the reactants. The effect that the external surface area of ZSM-5 zeolite crystals used

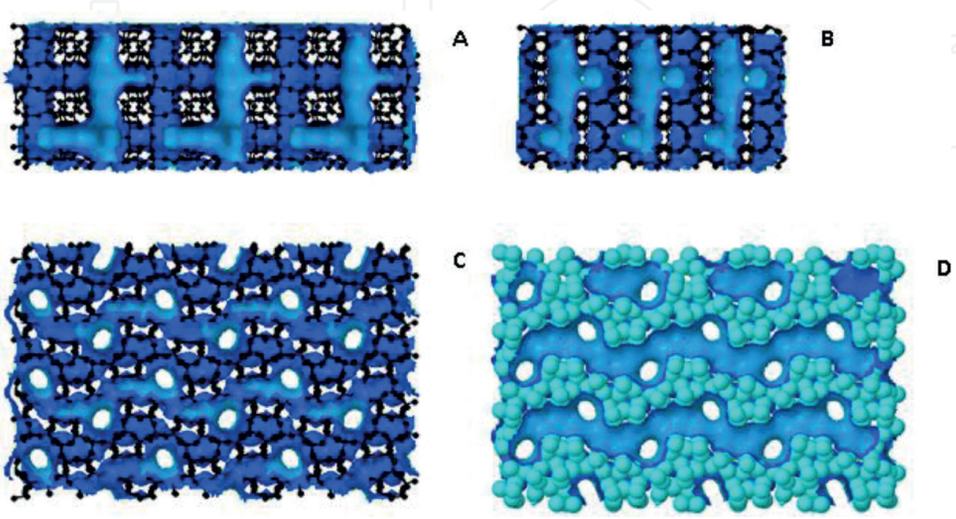

Figure 2. Front (A), right (B), and top (C) views of a "ball and stick" ZSM-5 (MFI) model; crosscutting of zigzag channels (D) of an "ionic radii" model; all from the IZA page: http://izasc.ethz.ch/fmi/xsl/IZA-SC/ftc_3d.php.

for shape-selective reactions causes, was reported previously [9]. Some authors in reported works have used the α_S-plot of Sing as alternative method to evaluate the external surface area and the true intra-crystalline capacity [10].

The aim of this study was to accurately describe the dependence of all the different types of ZSM-5 porosity on MR and to show which methods are best suited for measuring them in each range. This will allow us to develop an approach to the application of various existing methods of texture characterization for samples of zeolite with mixed porosity.

2. Methodology

A set of ZSM-5 zeolites in their sodium form (Na-ZSM-5) with a SiO_2/Al_2O_3 molar ratio (MR) varying from 30 to 120 was synthesized using a template of tetrapropylammonium bromide (TPABr) following the methodology reported by Ghiaci et al. [11]. Through the text and figures, these samples are called Z, followed by the MR value (30, 70, 95, or 120), for example, Z30 means an Na-ZSM-5 sample with an MR equal to 30. For comparison, a set of Na-ZSM-5 samples supplied by TOSOH Co., Japan, with MR 20, 23.3, and 30 were also studied. These TOSOH samples are called ZT, followed by MR value. A reference macroporous solid material required to estimate micropore volumes was obtained from the Tehuacan area in the state of Puebla, Mexico. This reference substrate was identified by X-ray powder diffraction (XRD) as α-SiO_2. X-ray powder diffraction of ZSM-5 samples was obtained in the 2θ ranges of 5–50 degrees using diffractometer Bruker D8, using nickel-filtered Cu Kα (λ = 0.154 nm) radiation. Scanning Electron Microscopy images were collected from a JEOL JSM-6610LV electron microscope with tungsten filament and an electron detector operated at 20 kV. N_2 adsorption isotherms were measured at the boiling point of liquid N_2 (76.4 K at the 2200 m altitude of Puebla City, México) in the interval of relative pressures, p/p^0 extending from 10^{-6} to 1 in an automatic volumetric adsorption system (Quantachrome AutoSorb-1C) in order to determine the textural parameters of ZSM-5 samples in addition to the evaluation of microporosity, which was analyzed through the determination of pore-size distributions calculated by the differential adsorption curves (DAC), Dubinin-Astakhov equation (D-A), and nonlocal density functional theory (NLDFT) approaches.

3. Results and discussion

3.1. X-ray analysis

The XRD patterns of all samples (**Figure 3**) are typical of ZSM-5 zeolites [12]. In general, all the samples showed reasonably sharp diffraction patterns, indicating good crystallinity. Please note that commercial TOSOH samples and those prepared in the laboratory are nearly identical. The main peaks appear at the following 2θ angles: 8.0°, 8.9°, 9.8°, 14.0°, 14.8°, 20.9°, 23.2°, 23.9°, 24.5°, 29.4°, and 30.0° (**Figure 3**). Most of these peaks are not resolved; usually, one peak is a superposition of several closely located reflections. For example, the [−101], [011], and

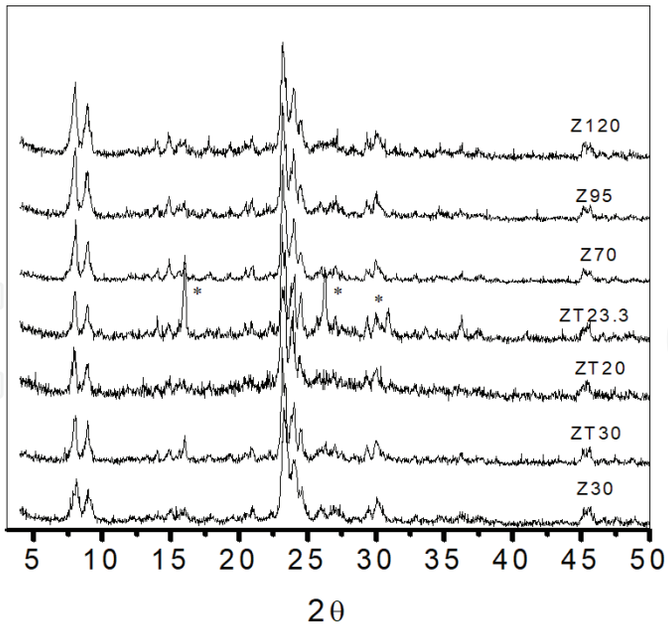

Figure 3. X-ray diffraction patterns.

[101] reflections positioned at 2θ = 7.92°, 7.93°, and 8.01°, respectively, gave rise to a total peak at ~8.0. The most important difference between the standard XRD pattern and the observed for both sets of samples is the relative intensity of the various peaks, but a detailed discussion of the changes in the structure of ZSM-5 due to MR variations and synthesis conditions is beyond the scope of the present work and will be discussed elsewhere. Three peaks that appear at 2θ = 16.0°, 26.4°, and 30.9° in the ZT23.3 sample (marked with asterisks) are most probably associated with an unidentified impurity.

3.2. Scanning electronic microscopy

In **Figure 4**, it can be seen that the effect of the templates used during the synthesis process affects the morphology of the zeolite crystals obtained. Thus, for example, in **Figure 4(a)** and **(b)** corresponding to zeolites ZT-20 and ZT-23.3, it can be seen that the crystals obtained have lath-like shapes. In the case of the ZT-30 and ZT-23.3 zeolites, clusters of spheroidal crystals are observed where the crystals of the zeolites coexist, as seen in **Figure 4(c)** and **(d)**. Finally, the SEM images of the zeolites ZT-30 and ZT-23.3 do not exhibit a predominant or defined geometry, as seen in **Figure 4(e)** and **(f)** [13].

3.3. High-resolution adsorption

N_2 sorption isotherms at 77 K for both sets of samples are shown in **Figure 5** as sorbed volume at standard temperature and pressure (STP) in cm^3 per gram of zeolite versus p/p^0. **Figure 5** shows the sorption isotherms using a logarithmic p/p^0 scale in the range of $10^5 \leq p/p^0 \leq 1$. The hysteresis loops shown by ZSM-5 zeolites are of the Type H3 or H4, characteristic of capillary condensation in the slit-like pores attributed to intercrystallite adsorption within aggregates. **Table 1** gives the values of some important parameters obtained from the analysis of isotherms.

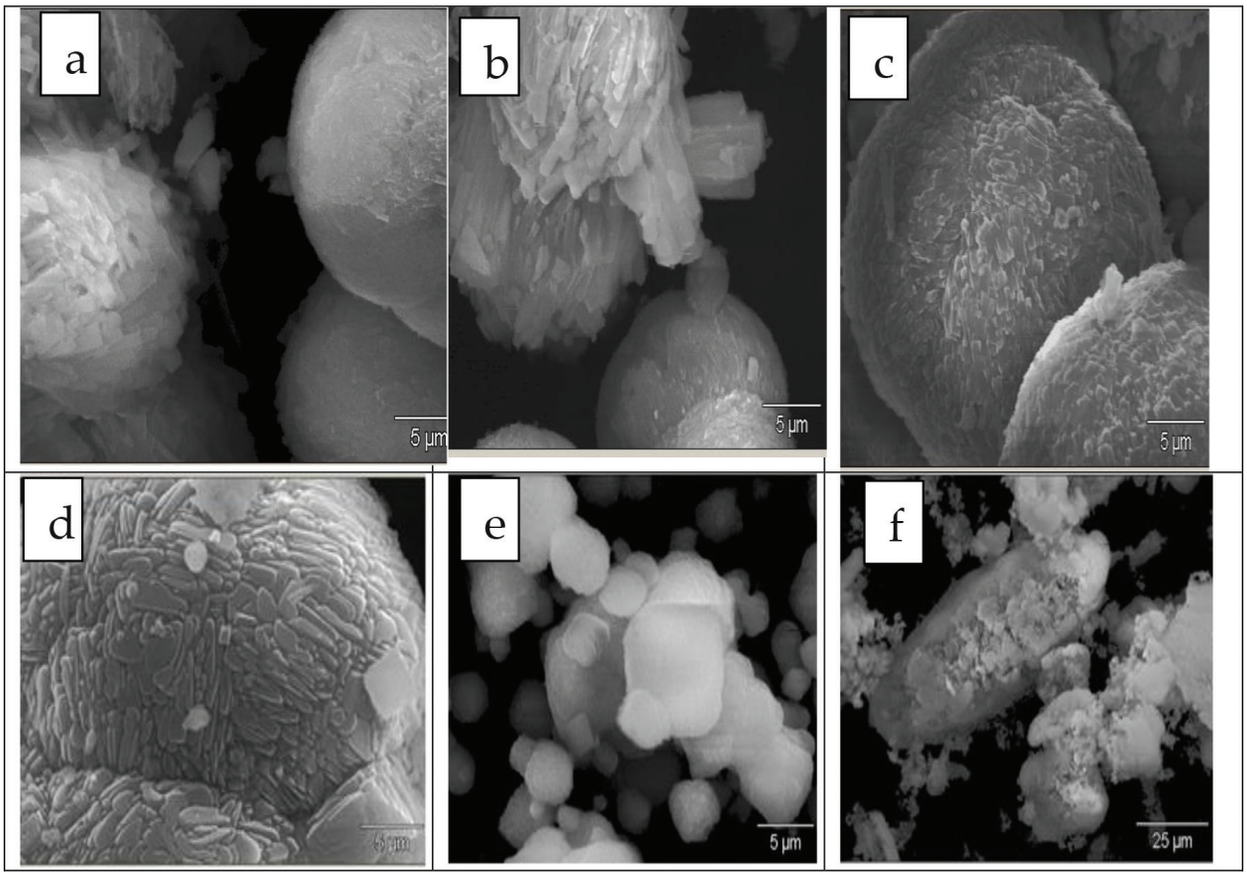

Figure 4. SEM images of ZSM-5 zeolite samples with different forms and crystal sizes: (a) ZT-20, (b) ZT-23.3, (c) ZT-30, (d) ZT23.3, (e) Z-30, and (f) Z-120.

All the N_2 isotherms are of Type I according to the IUPAC classification [14]. They indicate: (1) a high sorption at a very low relative pressure caused by the enhanced sorption potential of the ZSM-5 channel system and (2) formation of a monolayer at $0.1 \leq p/p^0 \leq 0.8$.

3.3.1. External surface area

To calculate the volume of the micropores from the sorption data, De Boer *t*-plots (thickness plots) and Harkins-Jura estimates are given in **Table 2**. An accurate estimate of these values can be influenced by the choice of the standard isotherm of a nonporous material selected to estimate the statistical thickness of the adsorbed layer (t) and the range of t values considered for the linear fitting [15] (**Figure 6**).

3.3.2. Microporosity

The total micropore volumes in $cm^3\ g^{-1}$ for all the samples are given in **Table 2**. These values were calculated from: (1) α_S-plots, (2) *t*-plots, and (3) the D-A equation (in this case, optimizing the values of the parameters n and E_0). The ratio of the micropore-filling capacity to the total sorption uptake, W_0/V_Σ, a parameter that somehow indicates the degree of crystallinity of the zeolite being analyzed, is also included in **Table 2** [16]. For the construction of the α_S and direct comparison plots, the adsorption volumes of the α-quartz without thermal processing

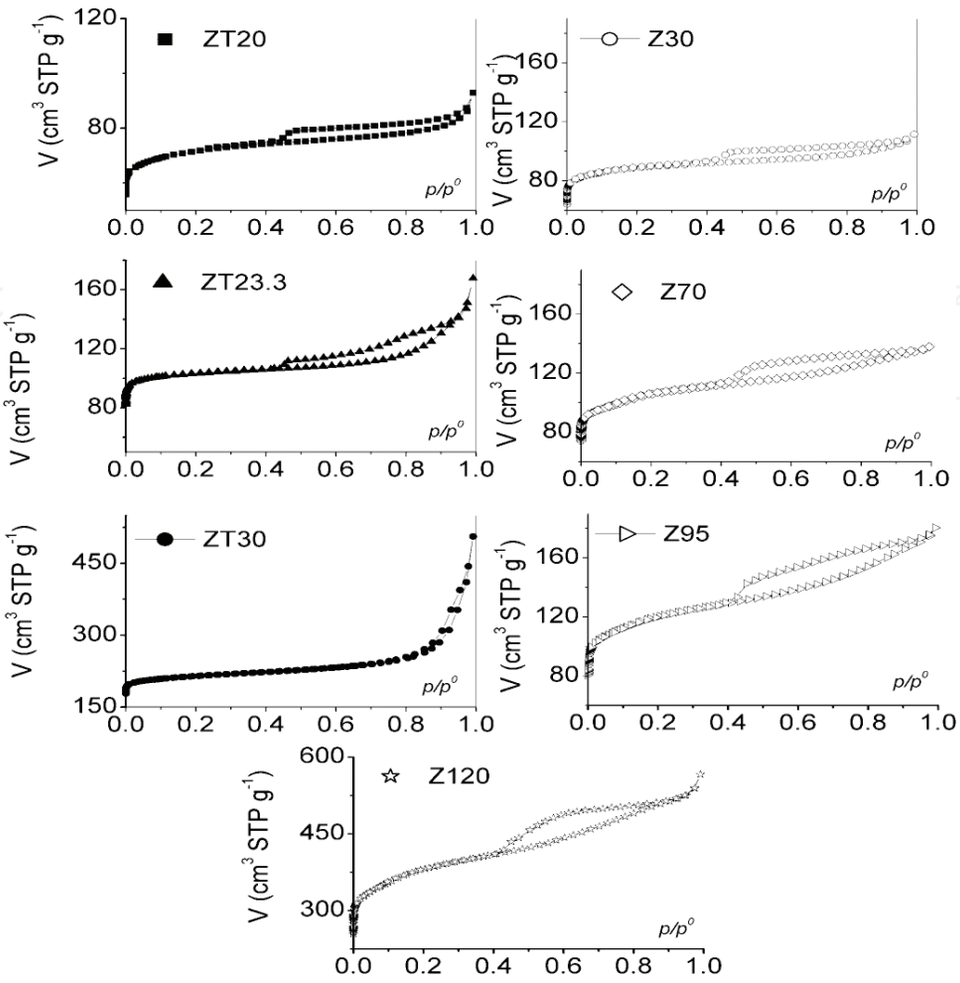

Figure 5. N_2 sorption isotherms at 77 K. For this figure and throughout, all samples supplied by TOSOH (ZT series) are designated by filled symbols, while samples synthesized for the present work (Z series) are designated by open symbols. The selection of symbols (circles, squares, etc.) is constant for all figures. Note that the ordinate scales are not always the same.

were used as reference values; α-quartz was chosen as a reference material, since adsorption on these substrata occurs similarly as on a flat surface; access to the underlying microporous structure is impeded by water molecules in the pore openings. The standard nitrogen

ZSM-5 zeolite	Si	Al	Na	O	Si/Al
Na-20	45.72	4.5	2.65	47.315	10.16
Na-23.3	47.313	3.61	2.58	46.496	13.10
Na-30	48.893	2.866	1.326	46.906	17.06
30	46.483	4.156	2.383	46.976	11.18
70	48.82	0.826	0.823	49.560	56.68
95	52.986	1.45	0.91	44.656	36.54
120	50.766	0.96	0.66	47.61	52.88

Table 1. ZSM-5 zeolite chemical composition (mass %, EDS).

Sample	A_{SL} ($m^2\ g^{-1}$)	A_{SB} ($m^2\ g^{-1}$)	A_E ($m^2\ g^{-1}$)	V_Σ ($cm^3\ g^{-1}$)	BET p/p^0 range	C_B	dp (nm)	W_0/V_Σ
ZT20	287.6	224.5	13.39	0.217	0.09–0.27	−56	3.866	33.179
ZT23.3	459.5	375.4	33.32	0.390	0.05–0.17	−244	4.155	26.153
ZT30	399.4	313.9	91.27	0.812	0.05–0.19	−202	1.034	25.738
Z30	533.6	409.0	19.72	0.129	0.05–0.19	−343	1.261	68.992
Z70	491.2	349.2	47.12	0.162	0.05–0.24	−110	1.855	63.580
Z95	562.3	397.0	83.41	0.207	0.05–0.27	−107	2.085	54.106
Z120	1784	1314	279.30	0.812	0.05–0.21	−276	2.471	54.451

Table 2. Adsorption structural parameters of ZSM-5 zeolites.

isotherms [17] are very similar to the adsorption isotherms of α-quartz along the adsorption branch up to a relative pressure of about 0.8. Since the same material was used as a reference for the α_S direct comparison plots, similar microporous volumes were obtained from all of these methods. However, *t*-plots give slightly different results because the reference isotherm corresponds to de Boer equation.

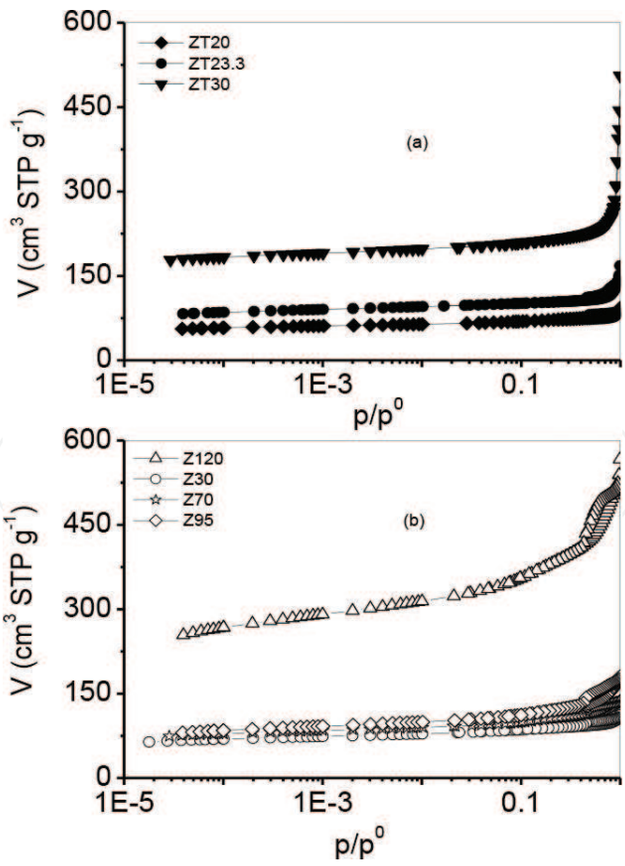

Figure 6. High-resolution N_2 sorption isotherms using a logarithmic p/p^0 scale. The graphs are divided in (a) and (b) parts with different scales due to the presence of higher values for most of the measured parameters for ZT30 and Z120 for this and the following figures.

A_{SL} is the Langmuir-specific surface area; A_{SB} is the BET-specific surface area; A_E is the external surface area; V_Σ is the volume sorbed at $p/p^0 = 0.95$; p/p^0 is the range used for the BET plot; C_B is the BET constant; *dp* is average particle diameter; and W_0/V_Σ is the degree of crystallinity.

3.3.2.1. High-resolution α_S-plots

The filling of macro, meso, and micropores can be proved by analyzing high-resolution α_S-plots starting at low relative pressures, that is, 10^{-5}; see **Figure 7**. There are some significant differences in the form of α_S-plots as a function of MR, mainly for Z120. A pronounced distortion of the isotherm shape is observed at a very low p/p^0, which can be explained by the enhancement of the sorbent-sorbate interaction in the pores of molecular dimensions, that is, the process of micropore filling [18]. This type of α_S-plot is characteristic of microporous adsorbents having a wide range of pore sizes and results in two or more separate stages of micropore filling. **Figure 7** shows three linear ranges. Region III, with $\alpha_S > 1.6$, corresponds to sorption in the mesopores and adsorption on the external surface of the zeolite. Extrapolation of the line to the ordinate at $p/p^0 = 0$ allows to estimate the total microporous volume W_0. Region II with $\alpha_S = 0.6–1.6$ can be a sorption in the porosity created by partial removal of the constituents of the zeolite matrix with the formation of structural defects. This type of porosity is typically developed by acid leaching. Region I, with $\alpha_S < 0.25$, is due to the stages of final filling of the volume of ultramicroporous elliptical sinusoidal channels (0.55 × 0.51 nm) and nearly circular straight channels (0.54 × 0.56 nm). This behavior is mainly due to the combined

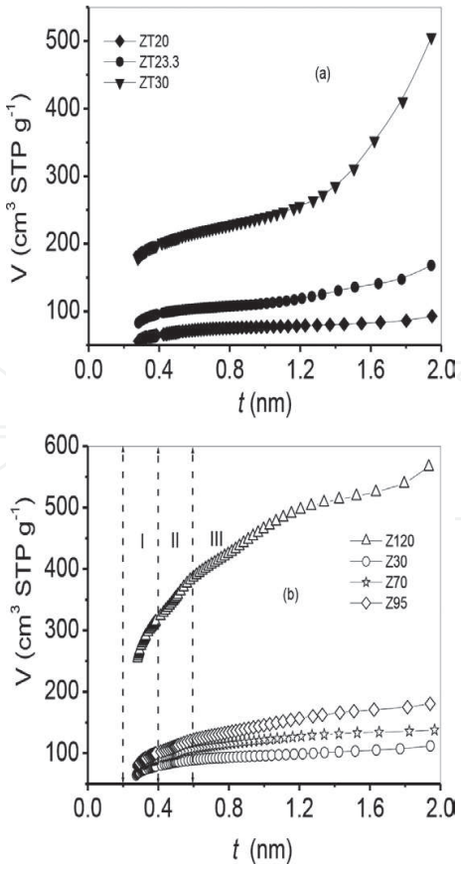

Figure 7. *t*-plots for the N_2 sorption isotherms.

filling of channels. However, this region is related to the filling of the ultramicropores corresponding to the narrowing and to the initial stages of channel filling. Zones of this α_S-plot for Z120 appear because the substratum has mesopores, supermicropores, and uniform micropores with elliptical and nearly circular free openings. The diameter of these channels corresponds to approximately 1–3 diameters of molecules. The micropore filling regions obtained through high-resolution plots for all samples are presented in **Table 2** (**Figures 8** and **9**).

3.3.3. Pore-size distributions calculated by the DAC, D-A, and NLDFT approaches

3.3.3.1. DAC method

Calculation of pore-size distributions from desorption branches of N_2 isotherms using the differential adsorption curves (DAC) [19] method yields bimodal distributions (**Figure 10**), with the thickness of the pore size of ca. 0.36 and 0.55 nm for all samples. The plots are unimodal with the pore ca. 0.36–0.40 nm. This approach correctly describes the essential qualitative features of N_2 sorption in the microporous zeolites, such as ZSM-5, that is, pores in the range of 0.3–0.6 nm. The results of these estimates are shown in **Table 3**.

3.3.3.2. D-A method

The pore-size distributions obtained by the D-A method [20] are shown in **Figure 11**. The average pore diameter, seen as a maxima on the curves by this method, varies according to

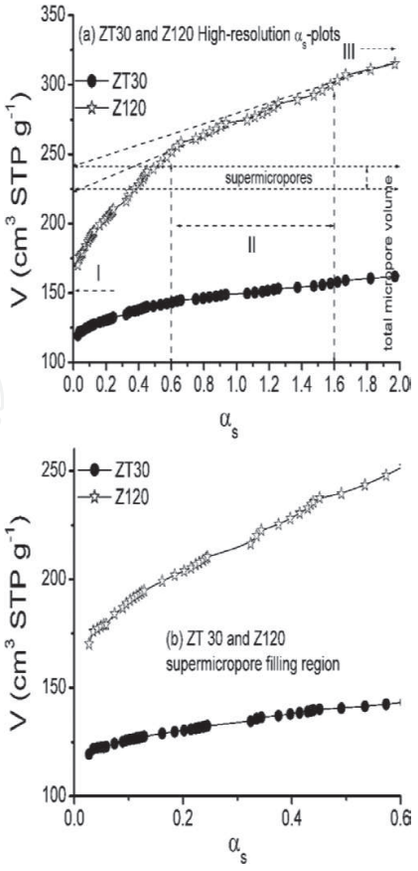

Figure 8. High resolution α_S-plot for N_2 sorption on ZT30 and Z120, showing (a) the ultramicropore and supermicropore volume regions and (b) the supermicropore linear region.

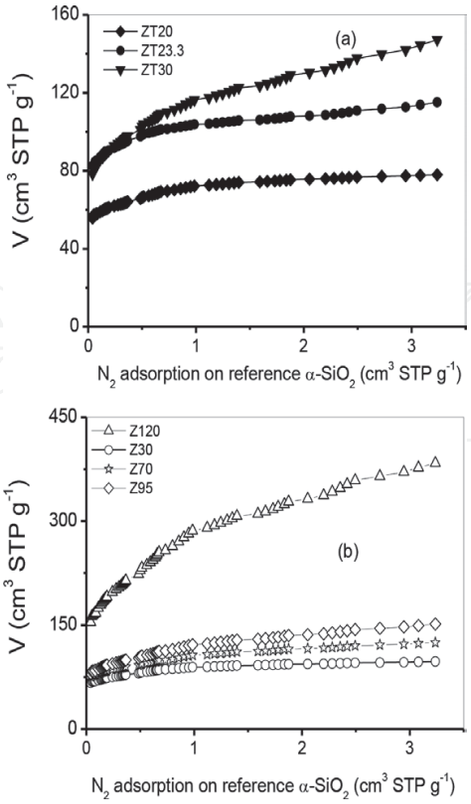

Figure 9. Comparative plots of the N_2 sorption isotherms versus adsorption using an α-SiO_2 reference.

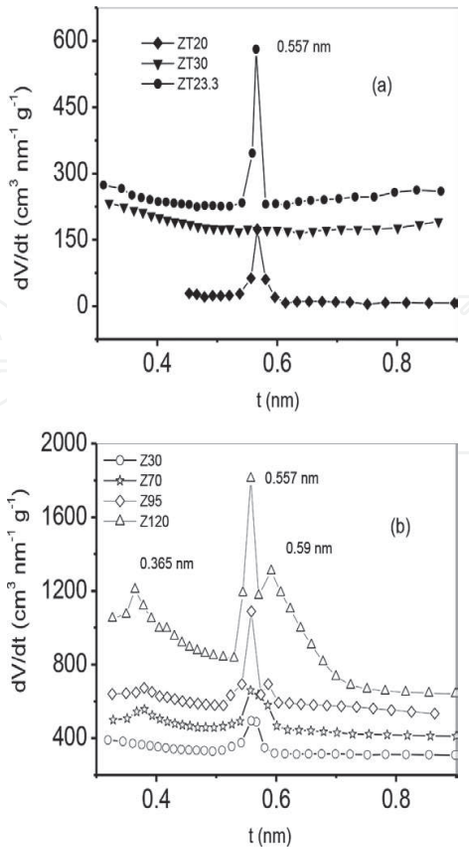

Figure 10. Micropore size distribution calculated from N_2 sorption isotherms using the DAC approach.

Sample	α_S	DAC	t	D-A	V_{meso}	E_0 (kJ mol^{-1})	n
ZT20	0.072	0.108	0.106	0.110	0.145	26.50	1
ZT23.3	0.102	0.131	0.147	0.165	0.288	20.50	1.3
ZT30	0.209	0.313	0.294	0.335	0.603	15.50	1.1
Z30	0.089	0.106	0.129	0.141	0.040	20.50	1.1
Z70	0.103	0.120	0.144	0.141	0.059	18.50	1
Z95	0.112	0.129	0.149	0.186	0.095	16	1
Z120	0.354	0.529	0.466	0.582	0.458	15.50	1

Table 3. Total micropore and mesopore volumes (W_0, V_{meso}, cm^3 g^{-1}) by various methods of analysis.

MR. **Table 3** lists the optimized W_0, n, and E_0 values using the D-A equation. The filling of elliptical channels of ZSM-5 with a length of 1.98 nm (width 0.51 × 0.57 nm) and connected through a zigzag path with a length of 0.665 nm (width 0.54) is the main contribution to the volume adsorbed. **Figure 11** shows ZSM-5 pore-size distributions obtained by the D-A method, assuming a cylindrical microporous channel; these plots provide average diameters very similar to the width of the porous cavities of the zeolites ZSM-5 (5th column of **Table 3**). The D-A results shown in **Table 2** suggest that MR in ZSM-5 zeolites promotes the opening and widening of their micropores. Nevertheless, the microporous volumes calculated from

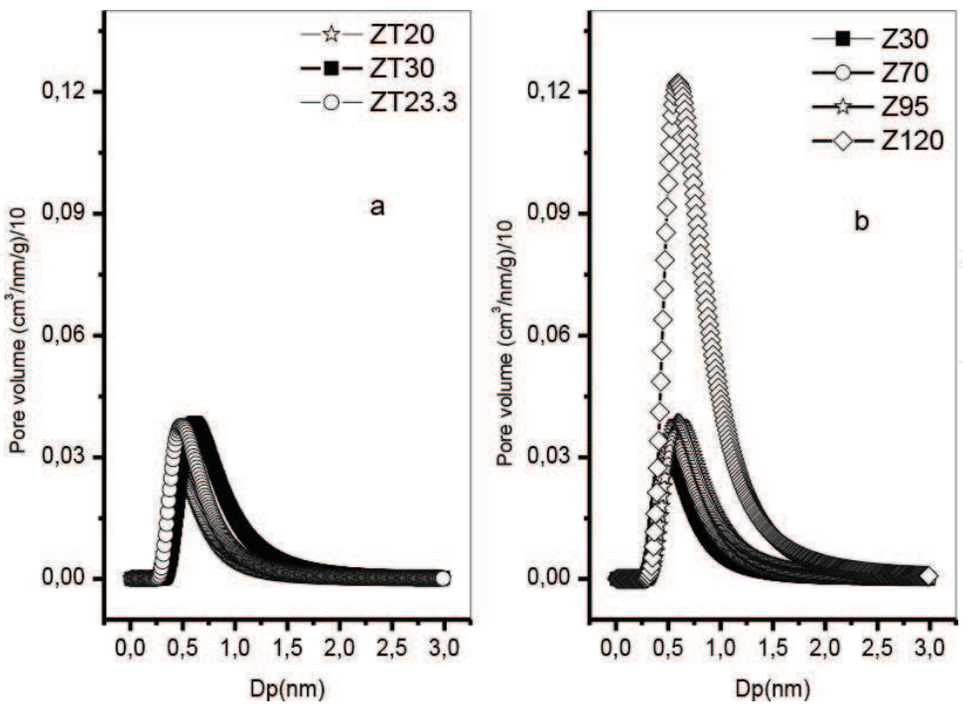

Figure 11. Micropore size distribution calculated from N_2 adsorption on the ZSM-5 zeolites through D-A approach.

the D-A equation are somewhat different from the microporous volumes calculated by the α_S and t methods. The fact that these D-A microporous volumes are always larger than the volumes calculated by the other methods suggests that the uptake at low relative pressures should be corrected for mesopore adsorption. This correction will result in a lower extrapolated value of the micropore volume from the D-A equation, and better agreement with other (α_S and t) methods will be reached. It can be seen there that the D-A treatment, while overestimating somehow the pore sizes, still provides an approximate estimate of the micropore volumes and their corresponding pore sizes. The E_0 values obtained by the D-A method decrease as MR increases: ZT20 > ZT23.3 > ZT30; Z30 > Z70 > Z95 > Z120 (**Table 2**). These values reflect

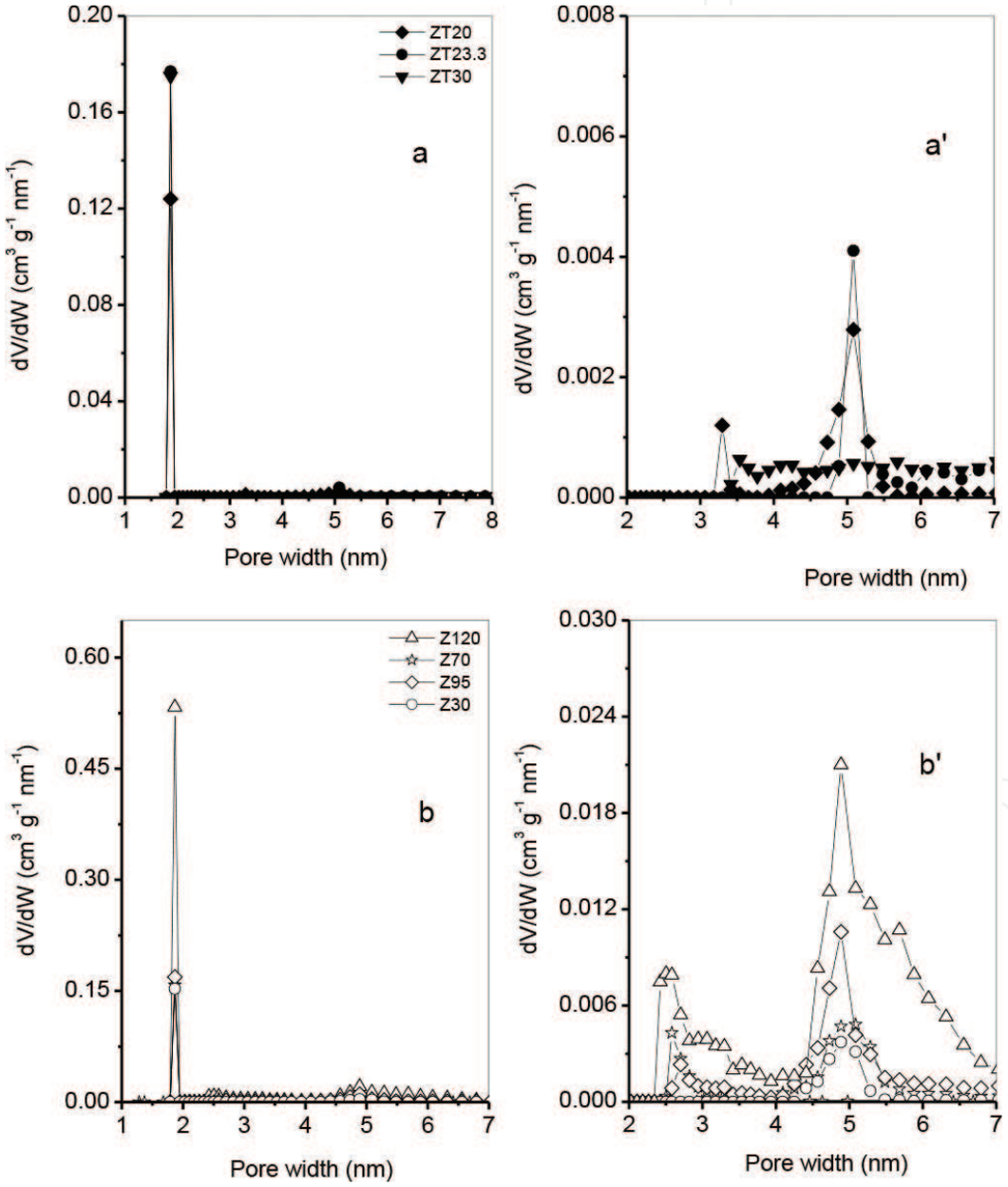

Figure 12. (a and b) NLDFT pore-size distribution showing the supermicropore region; (a′ and b′) close-up of the NLDFT pore-size distribution showing the supermicropore region on ZSM-5 zeolites.

Sample	DAC	D-A	NLDFT
ZT20	0.568	0.55	1.8/5.0
ZT23.3	—	0.57	1.8/5.0
ZT30	0.564	0.64	1.8
Z30	0.561	0.59	1.8/4.9
Z70	0.379/0.56	0.62	1.8/5.0
Z95	0.379/0.560	0.65	1.8/4.8
Z120	0.364/0.560/0.590	0.66	1.8/4.9

DAC is the differential curves of comparison plots method, D-A represents the Dubinin-Astakhov equation, and NLDFT is the nonlocal density functional approach.

Table 4. Pore diameter (nm) by different methods of analysis.

the dependence of this parameter on the SiO_2/Al_2O_3 ratio. Due to the crystalline nature of the zeolites, the force field created by the oxygen atoms in their structure must have symmetrical properties. Therefore, the E_0 values are affected by the aluminum content, which has changed some atoms of the zeolite framework in the channels to be displaced, as well as changing the sorption potential. From the comparison of the E_0 values obtained for these zeolites, this parameter is influenced not only by the pore sizes. Consequently, the Al content and the geometry of the pores have modified the electric field within the pores of the zeolites and thus have influenced the characteristic sorption energy.

3.3.3.3. Nonlocal density functional theory method

Nonlocal density functional theory (NLDFT) was developed to take into account pore sizes in voids of well-defined geometry [21]. With this approach, the molecules adsorbed in the pores tend to be packaged in accordance with the adhesion forces established with the substrate (i.e. attractive forces between adsorptive and adsorbent molecules) and interactions with the remaining fluid molecules. The molar density of the adsorbed phase varies as a function of pore size. The adsorption isotherm is calculated from a given pore shape (spherical, cylindrical, slit-like, etc.), and the experimental isotherm is given as the sum of a series of individual single-pore isotherms multiplied by their relative abundance over a range of pore sizes. In the present case, the microporous structure of ZSM-5 zeolite can be approximated as a bundle of parallel cylindrical pores and the nature of the adsorbent can be assumed as that of the silica. In this way, the distribution of supermicroporous zeolitic adsorbents can be calculated from high-resolution adsorption isotherms. The results of the analysis of the size of the supermicropores using the NLDFT method are shown in **Figure 12** and are listed in **Table 4**. The pore-size distributions obtained from the N_2 isotherms using the NLDFT cylindrical pore model yield bimodal distributions with pore size characteristics of 1.8 and 5.0 nm. It is observed from this figure

that the intensity of the distribution at 5.0 nm is poorly developed; however, it is represented in all distributions. A possible explanation is that the structures are not homogeneous and that it contains a significant amount of slit-like pores and pores of other irregular shapes. Based on the NLDFT method, one can get an idea about the actual widths and pore sizes of the supermicropore voids existing in ZSM-5 zeolites for which high-resolution N_2 isotherms are available.

α_S is Sing's α_S method, DAC is direct comparison plots, t is the t-plot employing the de Boer adsorption equation, D-A represents the Dubinin-Astakhov equation, V_{meso} is calculated by subtracting $W_{0\alpha S}$ from V_Σ (**Table 2**), E_0 is the characteristic energy of sorption, and n is the order of the sorption energy distribution from the Dubinin-Astakhov equation.

4. Conclusions

The obtained samples exhibit reasonable diffraction patterns, indicative of good crystallinity. The most important difference between the standard XRD pattern and those observed for both sets of samples is the relative intensity of the various peaks. The ZSM-5 samples synthesized are composed of crystals with different geometry in a range of sizes 5–10 μm. N_2 isotherms have been measured, starting at a relative pressure of 10^{-5} and up to 1. To evaluate the texture properties of ZSM-5 zeolites, BET, Langmuir, Ast, surface areas, and external surface area were used. A significant amount of micropores was found in all ZSM-5 zeolites. Such methods as α_S, t, and comparative plots (DAC) were used to estimate micropores in all zeolites. Nanopore size distributions (NSD) obtained from the N_2 adsorption at 77 K are in perfect agreement with the type of present pores for all the samples, that is, micropores, mesopores, and macropores. Thus, adsorption is probably the most sensitive tool for evaluating quality and structural properties of the microporous materials such as ZSM-5 zeolites. To characterize these nanomaterials, a combination of comparative methods based on reference isotherms on well-characterized ZSM-5 zeolites is recommended, as well as the results of DAC, D-A, and the NLDFT.

Acknowledgements

This work was partially supported by DGAPA-UNAM IN107817 Grant, VIEP, and the Academic Body "Investigación en zeolitas," CA-95 (PROMEP-SEP).

Conflicts of interest

The authors declare no conflict of interest.

Author details

Miguel Angel Hernández[1]*, A. Abbaspourrad[2], Vitalli Petranovskii[3], Fernando Rojas[4], Roberto Portillo[5], Martha Alicia Salgado[5], Gabriela Hernández[6], Maria de los Angeles Velazco[7], Edgar Ayala[7] and Karla Fabiola Quiroz[8]

*Address all correspondence to: vaga1957@gmail.com

1 Zeolites Research Department, Autonomous University of Puebla, Puebla, Mexico

2 Azad University of Shahryar-Shahre Ghods, Shahre Ghods, Tehran, Iran

3 Center for Nanoscience and Nanotechnology, National Autonomous University of Mexico, Ensenada, Mexico

4 Department of Chemistry, Autonomous Metropolitan University, Mexico City, Mexico

5 Faculty of Chemistry, Autonomous University of Puebla, Puebla, Mexico

6 Department of Chemical Engineering, Autonomous Metropolitan University, Mexico City, Mexico

7 Faculty of Chemical Engineering, Autonomous University of Puebla, Puebla, Mexico

8 Interdisciplinary Professional Unit of Biotechnology of the National Polytechnic Institute, Mexico City, Mexico

References

[1] MML RC, Russo PA, Carvalhal C, PJM C, Marques P, Lopes JM, Gener I, Guisnet M, Ribeiro FR. Adsorption of n-pentane and iso-octane for the evaluation of the porosity of dealuminated BEA zeolites. Microporous and Mesoporous Materials. 2005;**81**:259-267

[2] Kortunov P, Vasenkov S, Chmelik C, Karger J, Ruthven DM, Wloch J. Influence of defects on the external crystal surface on molecular uptake into MFI-type zeolites. Chemistry of Materials. 2004;**16**:3552-3558. DOI: 10.1021/cm0401645

[3] Remy MJ, Poncelet G. A new approach to the determination of the external surface and micropore volume of zeolites from the nitrogen adsorption isotherm at 77 K. The Journal of Physical Chemistry. 1995;**99**:773-779. DOI: 10.1021/j100002a047

[4] Rouquerol F, Rouquerol J, KSW S, Llewelyn P, Maurin G. Adsorption by Powders and Porous Solids. third ed. Amsterdam, The Netherlands: Academic Press; 2014. p. 495

[5] Matsumoto A, Zhao J, Tsutsumi K. Adsorption behavior of hydrocarbons on slit-shaped micropores. Langmuir. 1997;**1997**(13):496-501. DOI: 10.1021/10.1021/la9509581

[6] Sivasankar N, Vasudevan S. Adsorption of n-hexane in zeolite-5A: A temperature-programmed desorption and IR-spectroscopic study. The Journal of Physical Chemistry B. 2005;**109**:15417-15421. DOI: 10.1021/10.1021/jp0518714

[7] Cho HS, Miyasaka K, Kim H, Kubota Y, Takata M, Kitagawa S, Ryoo R, Terasaki O. Study of argon gas adsorption in ordered mesoporous MFI zeolite framework. Journal of Physical Chemistry C. 2012;**116**:25300-25308

[8] Ch B, Meier WM, Olson DH. Atlas of Zeolite Framework Types. 5th revised ed. Amsterdam, Netherlands: Elsevier; 2001. p. 213

[9] Sing KSW. The use of physisorption for pore structural characterization. In: Haynes JM, Rossi-Doria P, editors. Principles and Applications of Pore Structural Characterization. Bristol: Arrowsmith; 1985. pp. 1-11

[10] Lu X, Jaroniec M, Madey R. Use of adsorption isotherms of light normal alkanes for characterizing microporous activated carbons. Langmuir. 1991;**7**:173-177. DOI: 10.1021/acs.jced.6b01068

[11] Ghiaci M, Abbaspourad A, Arshadi M, Aghabarari B. Internal versus external surface active sites in ZSM-5 zeolite. Part 2: Toluene alkylation with methanol and 2-propanol catalyzed by modified and unmodified H_3PO_4/ZSM-5. Applied Catalysis A: General. 2006;**316**:32-46. DOI: 10.1016/j.apcata.2005.09.015

[12] Kawase R, Iida A, Kubota Y, Komura K, Sugi Y, Oyama K, Itoh H. Hydrothermal synthesis of calcium and boron containing MFI-type zeolites by using organic amine as structure directing agent. Industrial and Engineering Chemistry Research. 2007;**46**:1091-1098. DOI: 10.1021/ie060624z

[13] Sang S, Chang F, Liu Z, He C, He Y, Xu L. Difference of ZSM-5 zeolites synthesized with various templates. Catalysis Today. 2004;**93**:729-735. DOI: 10.1016/1.4943324

[14] Thommes M, Kaneko K, Neimark AV, Olivier JP, Rodriguez-Reinoso F, Rouquerol J, Sing KSW. Physisorption of gases, with special reference to the evaluation of surface area and pore size distribution (IUPAC technical report). Pure and Applied Chemistry. 2015;**87**:1051-1069. DOI: 10.1515/pac-2014-1117

[15] Hudec P, Smieskova P, Zidek Z, Schneider P, Solcova O. Determination of microporous structure of zeolites by t-plot method. State of the art. In: Aiello R, Giordano G, Testa F, editors. Studies in Surface Science and Catalysis. Vol. 142. Amsterdam, The Netherlands: Elsevier; 2002. pp. 1587-1602. DOI: 10.1021/la049817

[16] Hernández MA, Rojas F, Portillo R, Petranovskii V, Salgado MA. Influence of the Si/Al framework ratio on the microporosity of dealuminated mordenite as determined from N_2 adsorption. Separation Science and Technology. 2006;**41**:1907-1925. DOI: 10.1080/01496390600674901

[17] Sing KSW. Physisorption of nitrogen by porous materials. Journal of Porous Materials. 1995;**2**:5-8. DOI: 10.1007/BF00486564

[18] Sing KSW. Characterization of porous materials: Past, present and future. Colloids and Surfaces A: Physicochemical and Engineering Aspects. 2004;**241**:3-7. DOI: 10.1260/0144-5987.31.3.337

[19] Zhu HY, Lu GQ, Cool P, Vansant EF, Su BL, Gao X. Quantitative information on pore size distribution from the tangents of comparison plots. Langmuir. 2004;**20**:10115-10122. DOI: 10.1021/ja01145a126

[20] Stoeckli F, Lavanchy A, Hugi-Cleary D. Dubinin's theory: A versatile tool in adsorption science. In: Meunier FA, editor. Fundamentals of Adsorption VI. Amsterdam, The Netherlands: Elsevier; 1998. pp. 75-80. oai:doc.rero.ch:20080509175439-GP

[21] Astala R, Auerbach SM, Monson PA, Density Functional PA. Theory study of silica zeolite structures: Stabilities and mechanical properties of SOD, LTA, CHA, MOR, and MFI. The Journal of Physical Chemistry. B. 2004;**108**:9208-9215. DOI: 10.1021//jp0493733